Effects of Inertia Distribution on Regional Frequency Heterogeneity

EFFECTS OF INERTIA DISTRIBUTION ON REGIONAL FREQUENCY HETEROGENEITY

Zaichun Zhang[1], Robin Preece[1*]

[1]Department of Electrical and Electronic Engineering, The University of Manchester, Manchester, UK
**robin.preece@manchester.ac.uk*

Keywords: ELECTROMECHANICAL OSCILLATIONS, FAST FREQUENCY RESPONSE, FREQUENCY STABILITY, HETEROGENEITY, INERTIA DISTRIBUTION

Abstract

Heterogeneous inertia distribution can result in large regional frequency deviations and inter-area oscillations that exceed protection limits configured based on system-wide averaged performance. This paper examines how the spatial distribution of inertia affects frequency heterogeneity. An investigation into the effects of different fast frequency response (FFR) schemes on frequency heterogeneity is also presented. The frequency heterogeneity is quantified by calculating cosine similarity between regional frequency trajectories. The key results are obtained using a two-area model considering varying inertia distributions. A key finding is that the localness of regional frequency is independent of the inertia of a specific area, nor of the total system inertia. The inertia ratio, described as the ratio of the disturbance area inertia to that of the non-disturbance area, is shown to have a strong correlation with the frequency heterogeneity. It has been shown that generators are likely to be highly synchronous if the inertia ratio is greater than 2.5. Providing derivative FFR within the disturbance area always demonstrates benefits regarding frequency heterogeneity inhibition, whereas droop scheme typically introduces deterioration in frequency heterogeneity.

1. Introduction

Frequency stability has typically been studied using equivalent system models. Dynamics of all synchronous generators (SGs) are considered to be coherent during transients, represented by the centre of inertia (COI) frequency [1]. As converter interfaced generation (CIG) proliferates, the quantity of stored synchronous kinetic energy (i.e., *inertia*) within the system will no longer be a global variable and is instead heterogeneous, subjected to generation location and network topology [1]. Following major frequency events, the frequency deviation experienced around the network will vary considerably between areas. Areas that exhibit relatively low levels of inertia will experience faster change of frequency deviation and larger angular divergence with respect to neighbouring areas, leading to substantial power oscillations across inter-area ties [2]. System operators (SOs) will therefore experience difficulties with system- and regional-wide stability containment. This has encouraged research specifically concerned with the stability issues induced by heterogeneous inertia distribution.

Studies [3]-[5] are conducted using small (two- or three-area) test networks. An early study into the effects that large differences in regional inertia have on transient stability is presented in [3]. Increased angular separation between areas is shown when disturbances occur close to the low inertia area. The authors in [4], [5] explore how inter-area oscillations are affected by inertia distribution. It shows that in the presence of heterogeneous inertia distribution, fast and large flows of power will be transferred between areas. The effects of inertia distribution on large multi-area networks are examined in [6], [7]. A 16-machine 68-bus network is used in [6] for probabilistic frequency stability analysis, highlighting the limitations of using equivalent models in representing distinct locational frequencies. By using a reduced order Great Britain (GB) network, frequency stability assessment under varying regional inertia distributions is carried out in [7]. This work identifies protection issues induced by heterogeneous inertia distribution.

Implementing fast frequency response (FFR) to mitigate the stability issues induced by inertia heterogeneity has received recent attention. FFR schemes are usually designed to deliver large quantities of active power within milliseconds to a few seconds following major frequency events. Both *droop* response and *synthetic inertia* can be provided from the FFR devices, dependent on the control schemes applied [8]. With stability metrics as objectives, the problem has been formulated as optimisation problems as in [9], [10]. However, no consensus has been reached as these approaches may fail to reflect dynamics during large system transients whilst making simplifications of the network to ascertain optimised solutions.

Although studies to date have recognised regional variations in frequency, a systematic understanding of how the inertia distribution contributes to frequency heterogeneity is still lacking. Also, there has been no quantitative analysis of the extent to which the inertia distribution determines the localness of regional frequency. This paper establishes the relationship between inertia distribution and frequency heterogeneity considering varying inertia distributions. Also, how frequency heterogeneity is affected by different FFR schemes is analysed. This paper will help in safely resourcing inertia and FFR services in future systems. More importantly, it lays the groundwork for future research into the determination of regional inertia floors and regional FFR implementation requirements.

2. Theoretical Background

A common equation for describing rotor dynamics of SG is the swing equation as given by (1) – (3), where ω and $\Delta\omega$ are the

speed and speed deviation, ω_{syn} is the synchronous speed, τ_m and τ_e are the mechanical and electrical torque, τ_{net} refers to the net torque, P_m and P_e are the mechanical and electrical power, H is the inertia constant, and δ is the rotor angle divergence.

$$\tau_m = \frac{P_m}{\omega}; \quad \tau_e = \frac{P_e}{\omega} \tag{1}$$

$$\frac{d}{dt}\Delta\omega = \frac{1}{2H}(\tau_m - \tau_e) = \frac{\tau_{net}}{2H} \tag{2}$$

$$\frac{d}{dt}\delta = \Delta\omega = \omega - \omega_{syn} \tag{3}$$

Looking at (2) highlights that both H and τ_{net} are underlying factors in determining frequency deviation at a specific location (or a region) during transient events. In a multi-area network, not only does each area store a specific amount of inertial energy, but the τ_{net} experienced after disturbances is also different. This explains the reason why variations in regional frequency deviation are seen across the network. The unique oscillatory behaviour of the regional frequency means that SGs (or groups of SGs) are not accelerating (or decelerating) together. This leads to angular divergence between areas and power oscillations across inter-area ties.

These concerns may not prove to be prominent in conventional power systems as there is typically little variation in regional inertia. However, as CIG proliferates, it is possible for future systems to operate in the presence of large differences in regional inertia. In these instances, frequency events that occur within areas at lower inertia levels can incur higher regional rate of change of frequency (ROCOF) and larger changes in δ with respect to neighbouring areas, resulting in substantial power oscillations. Thus, future power systems are expected to be more vulnerable to issues associated with regional frequency stability, transient stability, and inter-area oscillations.

To illustrate how stability issues can be induced by inertia heterogeneity, two cases described in Table 1 are used. The results are generated using a two-area network which will be elaborated on further in Section 3. Area 1 initially exports power to Area 2 through an AC line. The values of H_{Area1} and H_{Area2} are determined on the same system base. Thus, the quantity of total inertial energy within a specific area can be described with respect to H and can be directly used for comparing cases. For both cases, the disturbance is implemented by disconnecting a non-synchronous generating unit in Area 2.

Table 1 Test case regional inertia constants

Test Case	H_{Area1}	H_{Area2}
Homogeneous	2.5 s	2.5 s
Heterogeneous	4 s	1 s

The *Homogeneous case* is representative of a condition when the total system inertia is evenly distributed across each area within the network. Whereas the *Heterogeneous case* represents a condition when low inertia area emerges (for example, due to CIG proliferation). Fig. 1 displays the trajectories of the system- and regional-wide frequency responses. Rotor angle separation ($\Delta\delta$) and active power flows through the AC tie (P_{tie}) are shown in Fig. 2.

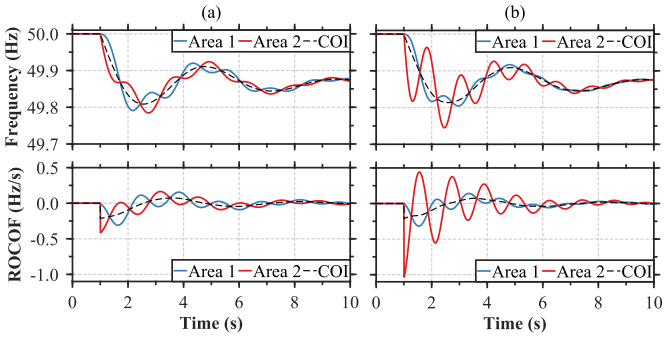

Fig. 1 Frequency responses: (a) *Homogeneous case*; (b) *Heterogeneous case*.

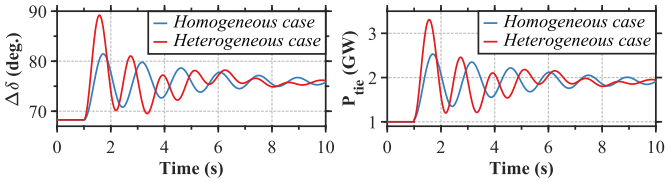

Fig. 2 Angular separation and tie line flows.

As the network operates with the same total system inertia, identical trajectories of the COI frequency are observed. Aspects where considerable differences have been observed include regional frequency, $\Delta\delta$, and P_{tie}. Viewing the frequency responses of Area 2 in Fig. 1, for the *Homogeneous case*, the initial ROCOF and the frequency nadir are at −0.417 Hz/s and 49.78 Hz respectively. For the *Heterogeneous case*, the initial ROCOF increases by 249% to −1.038 Hz/s, and the frequency nadir reduces by 0.03 Hz to 49.75 Hz. For this situation, there is a risk of generation tripping in practical systems due to violation of ROCOF-based protection limits. Fig. 2 shows that when the inertia distribution becomes heterogeneous, the system experiences larger and faster swings of $\Delta\delta$ and P_{tie} during transients. In practical terms, this might exceed transmission limits, causing cascading failures and even system blackouts.

The previous illustrative examples highlight that inertia distribution plays a vital role in affecting the frequency and angular stability of the power system. This is presented by looking at how regional frequency deviation (and hence $\Delta\delta$ and P_{tie}) is affected by varying inertia distribution. The next section will present a methodology which can be used to explore the extent to which the inertia distribution affects frequency heterogeneity. Once the relationship between inertia distribution and frequency heterogeneity is established, how FFR can be used to aid system operators in ensuring satisfactory system performance will be examined.

3. Methodology

In this section, a description of the test network used is presented. Following this, the technique used to quantify frequency heterogeneity is given. Modelling of FFR controls is also given. All modelling and simulations within this work are performed using DIgSILENT PowerFactory 2021.

3.1. Test network

A generic two-area system is used as the test network throughout this paper, as shown in Fig. 3. Each area in the network

consists of an SG and a load. The disconnection of a static generator (with no dynamic properties) at Bus 1 is used to unbalance the system. The two areas are connected via an AC transmission line. The network initially operates with high flows of power transferring from Area 1 to Area 2.

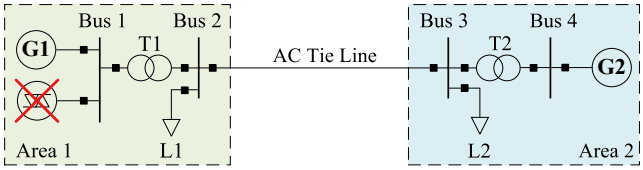

Fig. 3 Generic two-area test network.

The SG is represented by a 6th-order model with the dynamic parameters selected from [11] to represent CF1-HP gas-fired generator. Both SGs use the IEEE-DC1A exciter and operate with the GASTWD governor. A single type of SG (and supplementary SG control) is used at this stage in the research so that both SGs respond in a similar manner. Power system stabiliser is not implemented to help isolate the damping of the electromechanical oscillations as inherent system properties and not supplementary damping control. System loads use a ZIP model wherein the coefficients are selected based on [12].

The two SGs are equal in size. The sum of loads is equivalent to a typical summer loading condition in the GB system (36 GW). The disturbance is sized to 1,800 MW, equivalent to the Infrequent Infeed Loss Risk for the GB system. The AC tie line has an impedance of 2.25 + j22.5 Ω, representing the electrical distance between Scottish and English networks [13].

3.2. *Cosine similarity of frequency trajectories*

Quantification of frequency heterogeneity is needed in order to perform a systematic investigation into the impact of inertia distribution. In essence, to quantify frequency heterogeneity is to measure the similarity between frequency trajectories. Several methods currently exist for the measurement of trajectory similarity such as Euclidean distance, Hausdorff distance, cosine similarity, and Jaccard similarity [14]. In this research, cosine similarity is used as it is particularly useful for capturing and characterising oscillatory behaviour between trajectories.

Cosine similarity (CS) is defined as the cosine of the angle between vectors through the inner product [14]. A set of regional frequency trajectories of a power system with M regions can be described as $\mathbf{F} = \{\mathbf{F_1}, \mathbf{F_i}, \ldots, \mathbf{F_M}\}$. $\mathbf{F_i}$ is a $1 \times N$ vector and can be described as $\{f_{i,1}, f_{i,n}, \ldots, f_{i,N}\}$, in which N is the number of sampling points. The CS between the frequency of ith and jth region is defined as

$$\mathrm{Cos}(\mathbf{F_i},\mathbf{F_j}) = \frac{1}{N-1}\sum_{n=2}^{N-1}\frac{\overrightarrow{f_{i,n}\,f_{i,n+1}}\;\overrightarrow{f_{j,n}\,f_{j,n+1}}}{\left\|\overrightarrow{f_{i,n}\,f_{i,n+1}}\right\|\left\|\overrightarrow{f_{j,n}\,f_{j,n+1}}\right\|} \quad (4)$$

The value of CS is bounded in the range [–1, 1]. The closer CS is to 1, the more similar the two trajectories are. In the context of synchronous operation, a CS value closes to 1 indicates that SGs are highly synchronous during transients. Conversely, a CS value closes to –1 means that SGs are significantly oscillating against each other. Fig. 4 displays four pairs of typical regional frequency trajectories that lead to different values of CS. The results are generated using the two-area network.

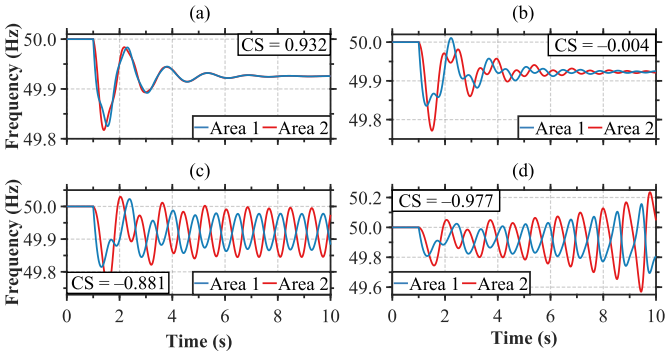

Fig. 4 Examples of regional frequency trajectories for different CS values: (a) highly synchronous; (b) moderate oscillation; (c) poorly damped stable oscillation; (d) growing oscillation.

3.3. *Simulation*

For the purpose of different inertia distribution creation, the H of both SGs is varied in the range [1, 4] s in 0.1 s steps. Assessing the impact of all combinations of regional inertia, leads to a total 961 simulations. The CS between the speed trajectories of the two SGs is calculated during each simulation. The length of the simulation is 10 s long with the underfrequency event occurring at 1 s. The sample size of 10 ms is selected – in total 900 sampling points for each trajectory.

3.4. *Fast frequency response (FFR) modelling*

In this research, regional concentrated grid-scale battery projects are considered as the FFR service provider. The battery energy storage system (BESS) model in PowerFactory is implemented to represent its dynamics [15]. Two types of FFR control schemes are considered including proportional (known as *droop*) control and derivative control (known as *synthetic inertia*). The two controller structures are displayed in Fig. 5.

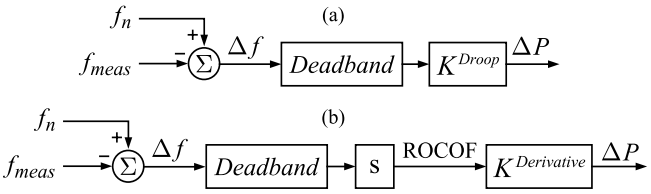

Fig. 5 Supplementary frequency controller: (a) droop controller; (b) derivative controller – adopted from [8].

The input of the frequency controller is the frequency deviation (Δf) which is the difference between nominal frequency (f_n) and locally measured frequency (f_{meas}). A dead band of ±15 mHz is implemented to prevent excessive operation of FFR around f_n. The droop controller differs from the derivative controller in terms of the signal that is input into the proportional gain (K^{Droop} and $K^{Derivative}$). The former acts on Δf whereas the latter acts on the rate of change of Δf (i.e., ROCOF). A basic derivative function block $F(s) = s$ is used in this research to enable inertial response emulation and the derivative is taken every time step of the simulation. It is acknowledged that designing a robust derivative controller is beyond the scope of this paper and, hence, practical difficulties associated with derivative control implementation as outlined in [16] are neglected. The output signal (ΔP) is sent to the outer active power control in the BESS which is subjected to a ramp limiter to represent the converter power ramp limitations.

The values of the proportional gains are taken from [17]. The capacity of FFR is sized to 1,400 MW, equivalent to the total requirements for the Dynamic Containment (DC) service procured by U.K. National Grid Electricity System Operator in 2021 summer [18]. It is necessary to clarify that the control scheme of the DC service is not implemented into the BESS.

4. Results & Discussion

This section presents the key results obtained from undertaking all combinations of regional inertia, including the ways in which different FFR schemes affect frequency heterogeneity.

4.1. Preliminary analysis

Preliminary analysis of the results for all scenario combinations is presented using the heat map shown in Fig. 6. The obtained 961 values of CS are laid out into a 31×31 matrix whose rows and columns are values of H_{Area1} and H_{Area2} respectively. Cells with the same CS value are connected by contours, representing the CS value in the range [–0.6, 0.9].

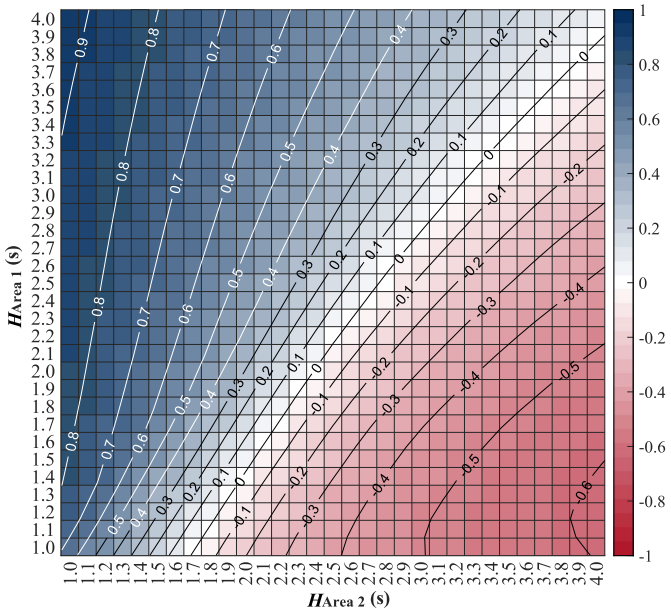

Fig. 6 Cosine similarity between regional frequency deviations.

The cells in the upper left of Fig. 6 represent regional inertia combinations that result in positive values of CS. Whereas the cells in the bottom right of the graph represent the combinations that result in negative values of CS. For each H_{Area1} (the disturbance area), the values of CS decrease with successive increases in H_{Area2} (the non-disturbance area). The greatest variation in CS is seen when H_{Area1} is equal to 1 s (as shown by the contours). The maximum value of CS (0.934) is seen when H_{Area1} = 4 s and H_{Area2} = 1 s, whereas the minimum value of CS (–0.606) is seen when H_{Area1} = 1 s and H_{Area2} = 4 s.

4.2. Correlation

It can be seen from Fig. 6 that the contours are close to linear. This might indicate a regional inertia combination equivalence with respect to CS, and the ratio (Φ_H) of the inertia of the disturbance area (H_{Area1}) to that of the non-disturbance area (H_{Area2}) is of concern. Fig. 7(a) displays the scatter plot of the relationship between Φ_H and CS. Also included for comparison is the relationship between H_{sys} and CS, as shown in Fig. 7(b). The Pearson correlation coefficient (ρ) as given in [19] is used to quantify how *linear* the relationship is between CS and inertia-based variables (i.e., Φ_H and H_{sys}).

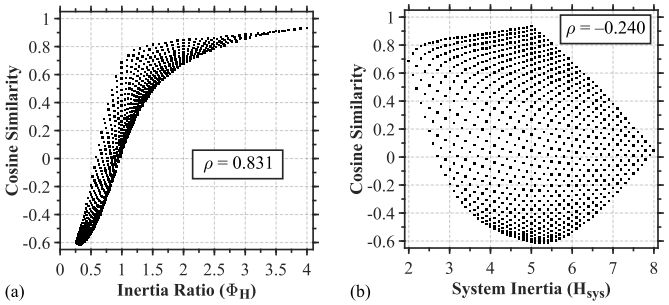

Fig. 7 Pearson correlation of cosine similarity with: (a) inertia ratio Φ_H; (b) system inertia H_{sys}.

A strong positive correlation between Φ_H and CS is seen (ρ = 0.831). Whereas no correlation is found between H_{sys} and CS (ρ = –0.240). This indicates that the extent of the localness of regional frequency is highly dependent on Φ_H, not the specific inertia of the disturbance area, nor the total system inertia. Broadly, the two areas are highly synchronous only when Φ_H is greater than 2.5 (all values of CS are greater than 0.8). Looking back to the heat map shown in Fig. 6 alongside the scatter plot shown in Fig. 7(a), it also indicates that homogeneous inertia distributions do not demonstrate significant advantages of inhibiting frequency heterogeneity. This is particularly true when the system operates at high inertia levels.

To clearly demonstrate the distinction in CS, four cases described in Table 2 are used. The two *Heterogeneous* cases result in the minimum and the maximum CS values respectively. The two *Homogeneous* cases are representing conditions when the disturbance area (and hence the system) exhibits the lowest and the highest level of inertia across all scenario combinations respectively. Fig. 8 presents the transient responses.

Table 2 Regional- and system-wide inertia, Φ_H, and CS

Case	H_{Area1}	H_{Area2}	H_{sys}	Φ_H	CS
Heterogeneous	1 s	4 s	5 s	0.25	–0.606
	4 s	1 s	5 s	4.00	0.934
Homogeneous	1 s	1 s	2 s	1.00	0.684
	4 s	4 s	8 s	1.00	0.048

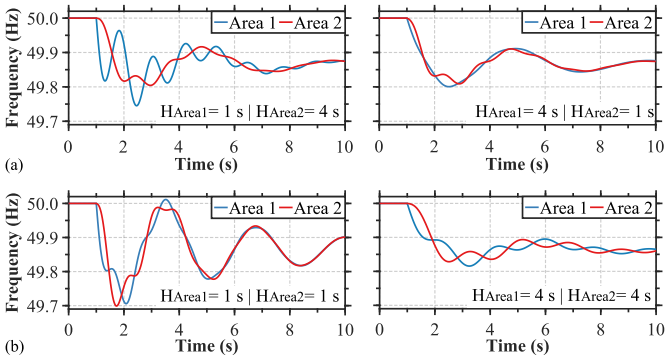

Fig. 8 Regional frequency deviations under different inertia distributions: (a) *Heterogeneous case*; (b) *Homogeneous case*.

Fig. 8(a) indicates that in the presence of heterogeneous inertia distribution, the system experiences notable variations in regional frequency only if the frequency event occurs in the low inertia area. This is because the corresponding SG will experience larger frequency deviations with respect to the high inertia area, governed by the swing equation. The resulting differences in regional frequency deviations thus lead to the minimum value of CS. Conversely, if the disturbance occurs in the high inertia area, then the disturbance-induced physical impact will be largely absorbed by the large rotating masses. Any difference in the regional frequency deviation is relatively small and generator speeds vary consistently during the event. This explains the reason why the resulting value of CS is close to 1.

The transient results shown in Fig. 8(b) highlight that homogeneous inertia distributions do not directly suggest a desirable system behaviour as persistent inter-area oscillations can be incurred when the system operates at high inertia levels. For the case when H_{sys} = 2 s, although both areas experience higher ROCOFs, the oscillation is adequately damped around 5 s after the event. When H_{sys} increases to 8 s, poorly damped but stable oscillations are seen (i.e., the transition from localness to homogeneity is comparatively slow in terms of regional frequency deviations). The smaller value of CS is seen in the case with H_{sys} = 8 s is hence explained.

4.3. Effects of FFR on frequency heterogeneity

The previous analysis reveals that the key to being able to inhibit large variations in regional frequency is to increase the quantity of inertial energy within the disturbance area. As FFR can be considered analogous to the inertial response of SGs, this subsection will ascertain if such a rapid power injection can mitigate frequency heterogeneity. To start with, a comparative analysis is given for the two possible FFR provision locations, Areas 1 and 2 in order to examine how the derivative scheme affects frequency heterogeneity. The derivative controller described in Section 3.4 is implemented into the BESS and two sets of CS values are obtained by undertaking all 961 scenarios detailed in Section 3.3. Fig. 9 compares the scatter plot of the relationship between Φ_H and CS. Also included for comparison is the *Base case* (i.e., cases with no FFR installed).

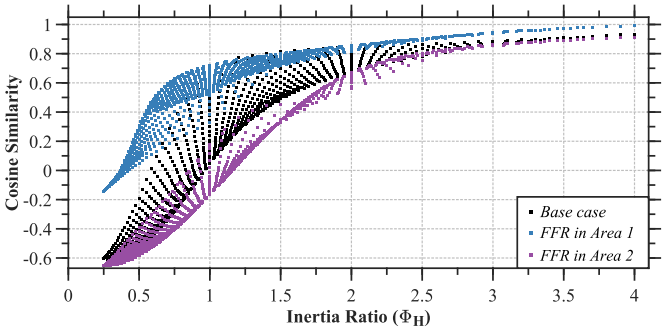

Fig. 9 Derivative scheme impacts on frequency heterogeneity.

The results shown in Fig. 9 indicate that derivative controller is capable of delivering energy in the inertial timeframe and hence, affecting the frequency heterogeneity. The FFR provision in Area 1 acts to increase the inertial energy within the disturbance area and hence, larger values of CS are seen compared to when no FFR is installed. Conversely, as the FFR provision in Area 2 increases the inertial energy within the non-disturbance area, smaller values of CS are seen. These findings support the previous notion that increasing the quantity of inertial energy within the disturbance area is advantageous and improves the system performance. Conversely, providing the synthetic inertia services within the non-disturbance area would risk the system stability, highlighting the necessity of allocating inertia-like frequency containment services in areas that could be susceptible to large power in-feeds.

Another comparative study is carried out to examine the capability of the droop scheme to inhibit frequency heterogeneity when the service is provided within the disturbance area. The droop controller described in Section 3.4 is implemented into the BESS and again, 961 simulations are performed to obtain values of CS. Fig. 10 compares the scatter plot of the relationship between Φ_H and CS, the *Base case* is included as well.

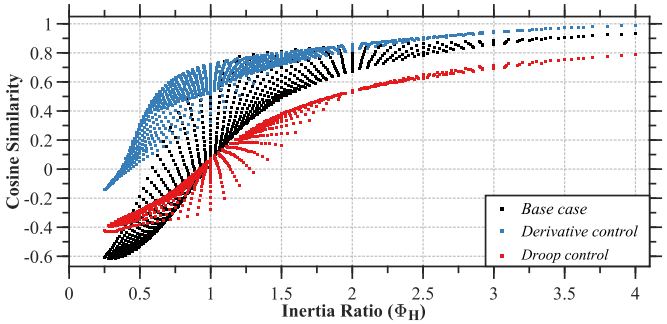

Fig. 10 Comparison between different FFR schemes on alleviating frequency heterogeneity.

For the vast majority of cases investigated, the provision of the droop based FFR leads to deterioration in frequency heterogeneity compared to when no FFR is installed. Although in some cases the values of CS are increased, the derivative scheme is always shown to provide a superior performance for frequency heterogeneity inhibition over the droop scheme. To demonstrate the difference in FFR behaviour during transients, a further comparative analysis is given. The results are generated for the case when H_{Area1} = 1 s and H_{Area2} = 4 s. Focus is paid to the impact of FFR (P_{FFR}) on τ_{net} within G1. Fig. 11 displays the transient responses. Note that occasional linear power injection is because the FFR control is subjected to a ramp limiter.

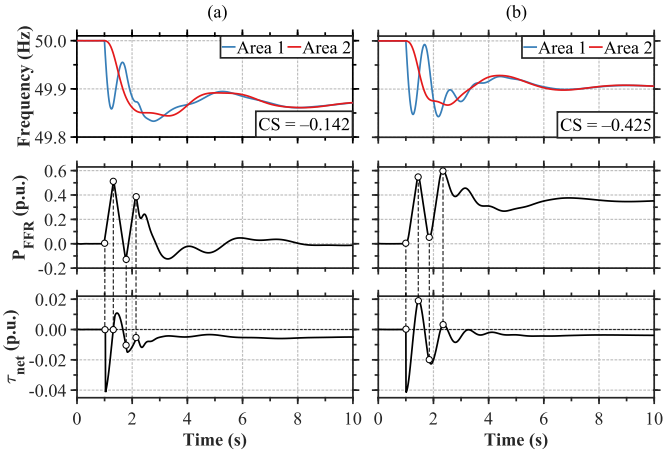

Fig. 11 Differences in FFR behaviour during transients: (a) derivative control; (b) droop control.

The CS value is increased to –0.142 with the derivative scheme applied (compared to –0.606 previously), whereas the CS is increased to –0.425 with the droop scheme applied. Looking back to the swing equation (2) and the derivative controller shown in Fig. 5(b), as ΔP is proportional to the ROCOF, injections of power are always delivered within the same time frame when τ_{net} is negative, as shown in Fig. 11(a). Consequently, the swings of τ_{net} are fully offset by the power injections. As shown in Fig. 11(b), although the battery starts to deliver power when the τ_{net} is negative, it is inevitable that sometimes injections of power coincide with the time when G1 experiences positive τ_{net} due to the droop controller output being proportional to Δf. The power injections hence further accelerate the rotor during each swing, aggravating the τ_{net} oscillation. This explains the reason why droop scheme provides limited benefit to the CS improvement, sometimes adversely.

5. Conclusions

This paper systematically examines how the inertia distribution affects frequency heterogeneity during underfrequency disturbance events. Cosine similarity (CS) is used to quantify frequency heterogeneity. It has revealed that the localness of regional frequency is largely independent of the specific area inertia and the total system inertia. The inertia ratio (Φ_H), described by the ratio of the disturbance area inertia to that of the non-disturbance area, is shown to have a strong positive correlation with CS. Regional inertia combinations that exhibit the same value of Φ_H demonstrate a similar degree of frequency heterogeneity. In this study, it has been shown that SGs are likely to be highly synchronous if Φ_H is greater than 2.5. In view of the induced persistent inter-area oscillations, homogeneous inertia distributions (i.e., when Φ_H =1) do not always lead to desirable system performance. This is shown to be true when the system operates at higher inertia levels.

Providing derivative based FFR within the disturbance area is shown to improve system performance which, conversely, implies that degradation in frequency heterogeneity occurs if such a service is delivered within the non-disturbance area. From a practical context, this highlights the high value of initiating frequency event disturbance location detection. Such a scheme could potentially be used to ensure that synthetic inertia services are delivered within the disturbance area. Unlike the derivative scheme, providing droop based FFR within the disturbance area rarely demonstrates benefits to frequency heterogeneity inhibition, owing to the inevitable overlaps in time between the rapid power injection and rotor acceleration.

Overall, this paper suggests that inertia-like frequency containment services should be incorporated into areas that could be susceptible to major power deficits (e.g., large interconnector or SG in-feeds). A natural progression of this work is to identify regional inertia floors and regional FFR procurement limitations to ensure a reliable operation of future power systems.

6. References

[1] F. Milano, F. Dorfler, et al.: 'Foundations and challenges of low-inertia systems (Invited Paper)', 20th Power Syst. Comput. Conf. Dublin, Ireland, June 2018, pp. 1–25

[2] D. Wilson, J. Yu, N. Al-Ashwal, et al.: 'Measuring effective area inertia to determine fast-acting frequency response requirements', Int. J. Electr. Power Energy Syst., 2019, 113, (February), pp. 1–8

[3] W. Bignell, H. Saffron, T. T. Nguyen, et al.: 'Effects of machine inertia constants on system transient stability', Electr. Power Syst. Res., 1999, 51, pp. 153–165

[4] A. Ulbig, T. S. Borsche, and G. Andersson.: 'Impact of low rotational inertia on power system stability and operation', IFAC Proc, 2014, 19, pp. 7290–7297

[5] T. S. Borsche, T. Liu, and D. J. Hill.: 'Effects of rotational Inertia on power system damping and frequency transients', in IEEE 54th Annual Conference on Decision and Control (CDC), 2015, pp. 5940–5946

[6] A. Adrees and J. Milanović.: 'Effect of load models on angular and frequency stability of low inertia power networks', IET Gener. Transm. Distrib., 2019, 13, (9), pp. 1520–1526

[7] X. Cao, I. Abdulhadi, A. Emhemed, et al.: 'Evaluation of the impact of variable system inertia on the performance of frequency based protection', 12th IET Int. Conf. Dev. Power Syst. Prot., 2014, pp. 1–6

[8] J. Fradley, R. Preece, M. Barnes.: 'VSC-HVDC for Frequency Support (a review) ', 13th IET Conference on AC and DC Power (ACDC), Manchester, UK, 2017.

[9] B. K. Poolla, D. Gross, and F. Dörfler.: 'Placement and implementation of grid-forming and grid-following virtual inertia and fast frequency response', IEEE Trans. Power Syst., 2019, 34, (4), pp. 3035–3046

[10] A. Scala, S. Pahwa, and C. Scoglio.: 'Optimal Placement of Virtual Inertia in Power Grids', IEEE Trans. Automat. Contr., 2017, 62, (12), pp. 1–10

[11] P. M. Anderson and A. A. Fouad: 'Power system control and stability' (Wiley India Pvt. Limited, 2008, 2nd edn.)

[12] A.Perez Tellez: 'Modelling Aggregate Loads in Power Systems', KTH Royal Institute of Technology, 2017

[13] Anaya-Lara, O., Hughes, F., Jenkins, et al: 'Influence of Wind Farms on Power System Dynamic and Transient Stability', 2006, Wind Engineering 30(2), pp. 107-127

[14] Z. Lin, F. Wen, Y. Ding, et al.: 'WAMS-Based coherency detection for situational awareness in power systems with renewables', IEEE Trans. Power Syst., 2018, 33, (5), pp. 5410–5426

[15] DIgSILENT PowerFactory, 'Application Example, Battery Energy Storing Systems', 2010, pp. 1–28

[16] E. Rakhshani, D. Remon, A. M. Cantarellas, et al.: 'Analysis of derivative control based virtual inertia in multi-area high-voltage direct current interconnected power systems', IET Generation, Transmission & Distribution, 2016, 10, (6), pp. 1458- 1469

[17] Francisco M.G and Jose L. R.: 'Modelling and Simulation of Power Electronic Converter Dominated Power Systems in PowerFactory' (Springer Press, 2020)

[18] 'Dynamic Containment', https://www.nationalgrideso.com/industry-information/balancing-services/frequency-response-services/dynamic-containment

[19] A. Edwards.: 'An Introduction to Linear Regression and Correlation', (W.H. Freeman, 1976, 2nd edn.)